Investigation of Lipid Organization in Biological Membranes by Two-Dimensional Nuclear Overhauser Enhancement Spectroscopy

Daniel Huster,[†,‡] Klaus Arnold,[‡] and Klaus Gawrisch*[,†]

Laboratory of Membrane Biochemistry and Biophysics, National Institute on Alcohol Abuse and Alcoholism, National Institutes of Health, 12420 Parklawn Drive, Room 158, Rockville, Maryland 20852, and Institute of Medical Physics and Biophysics, University of Leipzig, 04103 Leipzig, Germany

Received: August 20, 1998; In Final Form: November 2, 1998

The cross-peaks between lipid resonances in two-dimensional nuclear Overhauser enhancement spectroscopy ^{1}H NMR spectra, recorded with magic-angle spinning, contain valuable information about the structure and dynamics of the lipid bilayer. We have attempted a quantitative analysis of magnetization exchange between lipid resonances in the biologically relevant liquid crystalline lamellar phase. Spectra of 1,2-dimyristoyl-*sn*-glycero-3-phosphocholine (DMPC) water dispersions were recorded at mixing times from 0.005 to 1 s, and all diagonal and cross-peak volumes were determined by integration. The full relaxation-rate matrix was computed for the 10 lipid resonances by a matrix equation algorithm. Results of this mathematically rigorous approach were compared with simplified approaches to calculate cross-relaxation rates. In a second series of experiments, the DMPC was mixed with increasing amounts of perdeuterated DMPC-d_{67} to determine the percentage of intra- vs intermolecular magnetization transfer. With the exception of transfer between nearest neighbor protons by chemical bond, cross-relaxation in DMPC bilayers is exclusively intermolecular. There is no evidence for the transfer of magnetization over several bonds within lipid molecules by spin diffusion. Lipids exist in multiple conformations with rapid transitions between them, and, therefore, cross-relaxation rates do not represent stable molecular arrangements with fixed distances. Instead, the cross-relaxation rates reflect the probability of close approach between protons of neighboring lipid molecules. We established experimentally that cross-relaxation rates are proportional to the statistical average of lateral lipid−lipid contacts in binary mixtures. The location of lipid segments along the bilayer normal is best described by a distribution function. Segments which are located at the same depth in the bilayer approach each other with higher probability and have higher rates of magnetization transfer, compared with groups which are, on average, more distant and approach each other less frequently. The per-proton intermolecular cross-relaxation rates vary over the bilayer by only 1 order of magnitude, indicating surprisingly high probabilities of close approach even between the most distant groups, like the choline methyl groups and the terminal methyl groups of hydrocarbon chains. The results reflect the high degree of lipid motional disorder and the substantial variations in location of neighboring lipid molecules.

Introduction

The lipid matrix in biological membranes consists of a liquid crystalline lipid bilayer with partially ordered molecules. Lipids in membranes undergo rapid conformational transitions and perform rotational diffusion about the bilayer normal and lateral diffusion in the plane of the bilayer. The bilayer thickness fluctuates rapidly in space and time.[1,2] Location of specific lipid molecular groups along the bilayer normal is best described by broad distribution functions. In mixtures of several lipid species, membrane lateral organization may deviate from randomness, as seen in the formation of lipid domains and clusters. Although the fluid mosaic model of the lipid membrane,[3] established more than 25 years ago, describes the principal features of lipid organization in biomembranes, many important structural details have eluded investigation. The number of experimental parameters is still woefully inadequate to describe the multitude of lipid conformations, and more experimental input is needed to improve the membrane model. The aim of this study is to utilize nuclear Overhauser enhancement spectrocopy (NOESY) cross-relaxation rates between lipid protons for investigation of bilayer organization.

Oldfield's laboratory was the first to show that magic-angle spinning (MAS) experiments on membranes result in high resolution-like proton spectra of lipids.[4,5] The experiments require very little membrane material, on the order of 1 mg of lipid/sample. No intrusive sample preparation procedures, such as sonication of the lipid water dispersion with ultrasound to form small unilamellar liposomes, are needed. At high resonance fields, the lipid MAS centerband resonances are well resolved, with a typical peak line width of only 10−20 Hz. The good resolution and long spin−lattice relaxation times allow acquisition of two-dimensional NOESY spectra. Previous investigations raised concern because they reported intense cross-peaks between almost all lipid resonances.[6] The data suggest that even protons of lipid headgroups and the ends of hydrocarbon chains are in contact. This interpretation appears to be in conflict with the arrangement of lipids in stable bilayers.

* Phone: (301) 594-3750. Fax: (301) 594-0035. E-mail: gawrisch@helix.nih.gov.
† National Institutes of Health.
‡ University of Leipzig.

10.1021/jp983428h CCC: $18.00
Published on Web 12/10/1998

Consequently, the majority of investigators assumed that cross-relaxation rates in lipid membranes reflect not only close approach of lipid protons through space but also the relay of magnetization within lipid molecules by spin diffusion.[4,6−10] In this paper, we have quantitatively analyzed cross-relaxation rates between all lipid resonances, and we have determined the amount of intermolecular contributions to cross-relaxation. Our results prove that interactions between lipid protons, which are not nearest-neighbors by chemical bond, are exclusively intermolecular and that spin diffusion within lipid molecules does not contribute to cross-relaxation rates.

Interpretation of cross-relaxation data in lipid bilayers has little in common with interpretation of cross-relaxation data in soluble proteins. It is typically assumed that proteins are rigid with well-defined distances between protons. In contrast, lipid molecules are intrinsically flexible and change their conformation with correlation times from pico- to nanoseconds.[11] The distances to lipid segments of nearest-neighbor lipids in the bilayer change within nano- to microseconds.[12] Consequently, cross-relaxation rates are time averaged over an infinite number of lipid conformations and mutual arrangements of lipids. Despite all of the chaos, lipid molecules, on average, maintain their orientation in the bilayer, and membranes have a defined hydrophobic−hydrophilic interface. Because cross-relaxation is shown to be almost exclusively intermolecular, there is much to be learned about bilayer structure and dynamics from NOESY experiments. This paper is the first report of a full analysis of cross-relaxation rates in lipid membranes in terms of a dynamic bilayer structure.

Materials and Methods

Materials. The phospholipids 1,2-dimyristoyl-*sn*-glycero-3-phosphocholine (DMPC), 1-myristoyl-d_{27}-2-myristoyl-*sn*-glycero-3-phosphocholine (DMPC-d_{27}), and 1,2-dimyristoyl-d_{54}-*sn*-glycero-3-phosphocholine-1,1,2,2-d_4-*N*,*N*,*N*-trimethyl-d_9 (DMPC-d_{67}) were purchased from Avanti Polar Lipids, Inc. (Alabaster, AL), and used without further purification.

Sample Preparation. Lipid mixtures were prepared from chloroform solutions. The solvent was removed under a stream of argon. The lipid films were redissolved in approximately 500 μL of cyclohexane and frozen in liquid nitrogen. Samples were freeze-dried at a pressure of 50 μm of Hg for at least 4 h, resulting in a fluffy lipid powder. Dry lipid powder was hydrated with D_2O to a water content of 50 wt %, resulting in multilamellar vesicles. Lipid suspensions were stirred with a plastic rod, freeze−thawed, and centrifuged to equilibrate. Suspensions were transferred into 4-mm MAS rotor inserts made of Kel-F with a spherical sample volume of approximately 8 μL.

Nuclear Magnetic Resonance Spectroscopy. MAS NMR experiments were carried out on a Bruker DMX500 spectrometer (Billerica, MA). Samples were spun at frequencies of 2.5, 5.0, and 10.0 kHz using a Bruker double gas bearing MAS probe for 4-mm rotors operating with nitrogen gas. Proton experiments were carried out at a resonance frequency of 500.17 MHz, a spectral width of 3.3 kHz, and a 90° pulse length of 4 μs. Spin−lattice relaxation times, T_1, were measured by the inversion−recovery pulse sequence, and spin−spin relaxation times, T_2, by the Carr−Purcell−Meiboom−Gill pulse sequence.[13]

Two-dimensional NOESY experiments were carried out in the phase-sensitive mode.[14,15] The mixing time was varied between 0.005 s and 1 s. A total of 512 t_1 increments, with either 8 or 16 scans/increment at a relaxation delay of 4 s between scans, were accumulated yielding approximate acquisition times of 5 or 10 h/spectrum. The measurements were conducted at a temperature of 30 °C. The sample temperature inside the spinning rotor was calibrated by recording the main phase-transition temperature of DMPC and dipalmitoylphosphatidylcholine (DPPC) at the spinning speed of the experiment.

Determination of NOESY Cross-Relaxation Rates. Experimentally measured NOESY diagonal peak and cross-peak volumes at mixing time t_m, represented by the peak volume matrix $\mathbf{A}(t_m)$, and the cross-relaxation rates between diagonal peaks, represented by the relaxation-rate matrix **R**, are linked by the matrix equation

$$\mathbf{A}(t_m) = \exp(-\mathbf{R}t_m)\mathbf{A}(0) \tag{1}$$

where $\mathbf{A}(0)$ is the peak volume matrix at mixing time zero.[16−18] **R** for *N* magnetically nonequivalent spins is

$$\mathrm{R} = \begin{pmatrix} \rho_{11} & \sigma_{12} & \sigma_{13} & \cdots & \sigma_{1N} \\ \sigma_{21} & \rho_{22} & \sigma_{23} & & \\ \sigma_{31} & \sigma_{32} & \rho_{33} & & \vdots \\ \vdots & & & \ddots & \\ \sigma_{N1} & & \cdots & & \rho_{NN} \end{pmatrix} \tag{2}$$

where σ_{ij} represents cross-relaxation rates and ρ_{ii} represents effective relaxation rates of the diagonal peaks. According to the convention, σ_{ij} is the cross-relaxation rate of magnetization transfer from spin *j* to *i*, and σ_{ji} of transfer from spin *i* to *j*. The effective relaxation rate, $\rho_{ii} = R_{ii} - \sum\sigma_{ji}$ ($j = 1, .., N$), where R_{ii} is the spin−lattice relaxation rate of the diagonal peaks. The relaxation-rate matrix is not symmetrical if the number of magnetically equivalent spins per resonance varies. However, there is symmetry in the per proton transfer rates, and the cross-relaxation rates satisfy the symmetry condition

$$n_j\sigma_{ij} = n_i\sigma_{ji} \tag{3}$$

where n_j and n_i are the number of spins in resonances *j* and *i*, respectively.

At a fixed mixing time, **R** is calculated by rewriting eq 1 in terms of the matrix of eigenvectors, **X**, and the diagonal matrix of eigenvalues, **D**, of the normalized peak volume matrix $\mathbf{a}(t_m) = \mathbf{A}(t_m)\ [\mathbf{A}(0)^{-1}]$,[16−18] resulting in

$$\mathbf{R} = -\frac{\mathbf{X}(\ln \mathbf{D})\mathbf{X}^{-1}}{t_m} \tag{4}$$

For the determination of **R**, the diagonal peak and cross-peak volumes of NOESY spectra were determined by a process of iterative segmentation using the program AURELIA (Bruker Analytische Meβtechnik GmbH, Rheinstetten, Germany). Segmentation starts at the top of each peak and advances down recursively until data points of other peaks or the baseline level are reached.

The computation of the relaxation-rate matrix according to eq 4 was carried out on a PC using Mathcad software (MathSoft, Inc., Cambridge, MA). For the calculation of **R**, a volume matrix $\mathbf{A}(t_m)$ with maximal cross-peak volumes (t_m = 150−500 ms) was chosen. The peak volume matrix $\mathbf{A}(0)$ at "zero" mixing time was approximated by a measurement at the very short mixing time of 5 ms. These data points are more reliable than those measured with back-to-back pulses at true mixing time zero.

Alternatively, cross-relaxation rates were calculated according to the spin-pair interaction model.[16,19] This approach assumes that the complex multispin problem is decoupled and can be

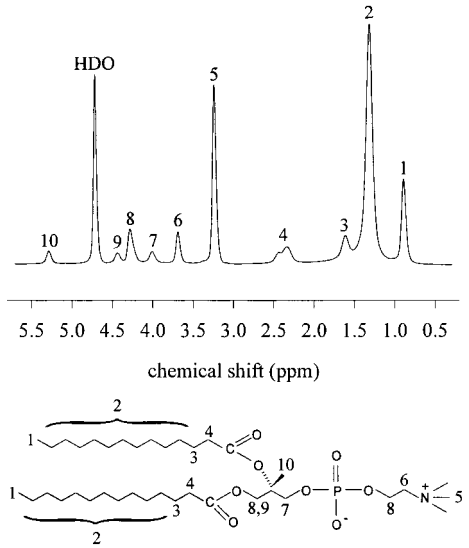

Figure 1. 500 MHz ^{1}H magic-angle spinning NMR spectrum of DMPC in 50 wt % D_2O recorded at a MAS spinning speed of 5 kHz and a temperature of 30 °C. The numbers on the DMPC structure refer to the peak assignments of proton resonance peaks.

treated as a series of two-site exchanges. With this assumption we obtain

$$A_{ii}(t_m) = [A_{ii}(0)/2][1 + \exp(-2\sigma_{ij}t_m)] \exp(-t_m/T_{ii}) \quad (5a)$$

for the diagonal peak volumes and

$$A_{ij}(t_m) = [A_{jj}(0)/2][1 - \exp(-2\sigma_{ij}t_m)] \exp(-t_m/T_{ij}) \quad (5b)$$

for the cross-peak volumes. The variables, $A_{ii}(t_m)$ and $A_{ij}(t_m)$, are the respective diagonal peak and the cross-peak volumes at mixing time t_m, and $A_{ii}(0)$ and $A_{jj}(0)$ are the diagonal peak volumes at mixing time zero. The values $1/T_{ii}$ and $1/T_{ij}$ define a rate of magnetization leakage toward the lattice. The diagonal peak volumes at time point zero were calculated from the fit of diagonal peak intensities to eq 5a. Cross-relaxation rates were obtained from fits of experimental cross-peak volumes at varying mixing times to eq 5b, using the $A_{jj}(0)$ values from the previous fit. Calculations were conducted using the nonlinear regression curve fitter in Sigmaplot (Jandel Scientific Software, San Rafael, CA).

To analyze NOESY data obtained at one short mixing time, eq 5b was simplified further by expansion of the cross-relaxation exponential term into a Taylor series which was truncated after the linear term, yielding

$$\sigma_{ij} = \frac{A_{ij}(t_m)}{A_{jj}(t_m)\, t_m} \quad (6)$$

The exponential decay of cross-peak intensity due to spin−lattice relaxation was considered by substituting $A_{jj}(0) \times \exp(-t_m/T_{ii})$ by the diagonal peak volume $A_{jj}(t_m)$ measured at the mixing time t_m.

Results

Signal Intensities in the MAS Centerband. MAS collects proton NMR resonance intensities into center- and sidebands which are separated from each other by multiples of the rotor spinning speed. In Figure 1, the centerband of the ^{1}H NMR spectrum of DMPC hydrated with an excess of D_2O is shown (see Table 1 for signal assignment). The intensity distribution between side- and centerbands depends on resonance signal broadening by dipolar proton−proton interactions. Protons in the lipid glycerol groups and upper hydrocarbon chains experience strong dipolar interaction with nearest-neighbor protons, and their resonances have a significant amount of intensity in the MAS rotational sidebands. In contrast, resonances of protons with weak dipolar interaction have negligible sideband intensity, e.g., the resonances of the choline headgroups and of the methyl groups of hydrocarbon chains (Figure 2). As a result, resonance signal intensity in the centerband for some of the peaks is not proportional to the number of contributing protons. With higher MAS spinning speed, the sideband intensities decrease and the ratio of peak intensities within the centerband is closer to the ratio of protons contributing to the resonances.

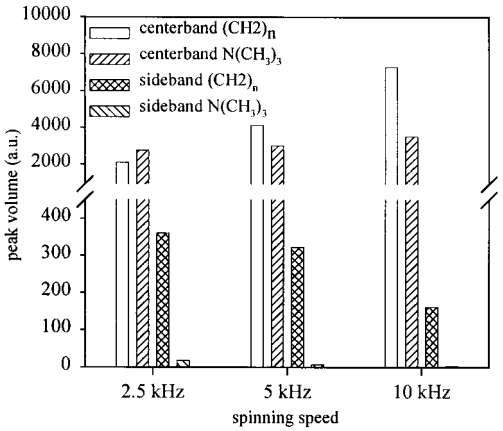

Figure 2. Dependence of MAS center- and sideband peak intensities on MAS spinning speed. Increasing spinning speed gathers intensity into the centerband while sideband peaks decrease in intensity.

Spin−Lattice Relaxation Rates. The relaxation data of all resonances could be approximated well by a single exponential decay within experimental error. For the chain methylene resonance (1.30 ppm), this is somewhat surprising, because a large number of protons with potentially different relaxation rates are contributing to it. Rate differences are expected because of the order parameter and correlation time gradients along lipid hydrocarbon chains, with chain segments in the bilayer center more disordered than those near the glycerol.[20] Apparently, the individual relaxation rates are close and cannot be resolved considering the limited precision of measured signal amplitudes.

Nevertheless, the existence of differences in chain proton relaxation rates is likely and may cause the changes in spin−lattice relaxation rates as a function of MAS spinning speed (Table 1), detected for peaks with relatively high sideband intensities. The sideband signals contain a disproportional amount of magnetization from protons with strong dipolar interaction with neighboring protons, which are also likely to experience different spin−lattice relaxation rates. With increasing spinning speed, spectral density is redistributed from the sidebands to the centerband, resulting in an apparent dependence of spin−lattice relaxation rates on spinning speed.

Spin−spin relaxation times T_2 are significantly shorter than T_1 relaxation times and reasonably close to apparent T_2 values estimated from the line width of centerband resonance peaks. This indicates that resonance lines of the MAS centerband are homogeneously broadened, with little room for improvement of resolution by better shimming.

Cross-Relaxation Rates. Cross-relaxation rates can be determined in NOESY and rotating-frame Overhauser enhancement spectroscopy (ROESY) experiments. The ROESY experiment has the advantage of being less vulnerable to transfer of

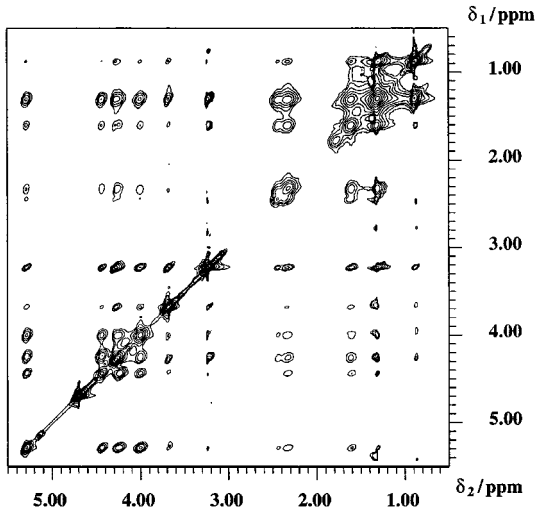

Figure 3. 2D NOESY contour plot of the DMPC (50 wt % in D_2O) MAS centerband resonances. The spectrum was recorded at a MAS spinning speed of 5 kHz, a mixing time of 300 ms, and a temperature of 30 °C. Data were recorded in a phase-sensitive mode. All cross-peaks have positive intensity.

magnetization within a molecule by spin diffusion.[21] However, application of ROESY is severely limited by the very short spin relaxation times of lipid proton resonances in the rotating-frame coordinate system, $T_{1\rho}$, that are approximately equal to T_2 (see Table 3). During the mixing time of the NOESY experiment, the magnetization decays with the much longer spin−lattice relaxation times T_1, which results in less signal attenuation and higher precision of cross-relaxation rates.

From the sign of NOESY cross-peaks (Figure 3), the order of magnitude of motional correlation times, which are responsible for cross-relaxation, can be estimated. All cross-peaks had positive intensity, indicating that these correlation times are longer than 0.36 ns (isotropic tumbling motions assumed). Cross-relaxation rates between all lipid resonances were calculated assuming that magnetization underneath each peak can be treated as one entity with uniform relaxation parameters. Rates were calculated using three mathematical approximations. (i) *Matrix approach*: The magnetization underneath each peak was measured at mixing times of 0.005 and 0.15−0.5 s, and relaxation rates were calculated by matrix equation (4). Magnetization of multiple protons contributing to one resonance is treated as uniform. This procedure accounts for cross-relaxation between all resolved peaks and their mutual interference. The precision of the approach depends on the experimental errors of the elements in the peak volume matrices $\mathbf{A}(0)$ and $\mathbf{A}(t_m)$. Precision of the calculated relaxation-rate matrix was confirmed by comparing measured and calculated peak volumes for at least six more mixing times. (ii) *Pair interaction approach*: The magnetization underneath each peak was measured as a function of six to eight mixing times in the range from 0.005 to 1 s. The mixing time dependence of pairs of diagonal peaks and of the cross-peak between them were approximated by the pair interaction equations (5a,b). The determination of cross-relaxation rates by nonlinear regression, using data points obtained at all mixing times, improves the precision of calculated cross-relaxation rates. However, the procedure treats all spins as isolated spin pairs, and the limits in cross-relaxation rate precision related to this assumption must be explored. (iii) *Single mixing time approach*: Cross-peak and diagonal peak intensities are determined at one relatively short mixing time. Cross-relaxation rates are calculated according to eq 6. This approach requires the least effort in data acquisition and analysis. However, it considers only pair interactions and makes simplifying assumptions regarding the mixing time dependence of cross-peak intensity.

Figure 4 presents the data calculated by the matrix approach. Experimentally determined peak volumes of all diagonal peaks and cross-peaks as a function of mixing time are shown as data points. The lines are the fit to these intensities using the parameters determined by the matrix approach. The calculated relaxation rates obtained at MAS spinning speeds of 5 kHz and higher fit all measured peak volume matrices over the mixing time range from 0.005 to 1 s, indicating that the experimental error in the measured peak volumes is small. Table 1 compares spin−lattice relaxation rates, R_i, calculated by the inversion−recovery experiment with those of diagonal peaks in the NOESY spectra, calculated by the equation $R_{ii} = \rho_{ii} + \sum\sigma_{ji}$ ($j = 1, .., N$). The agreement for MAS spinning speeds of 5 kHz and higher is excellent, confirming the consistency of data calculated by the matrix approach. Peak volumes calculated at the lower spinning speed of 2.5 kHz are less reliable because of significant amounts of signal intensity in MAS sidebands. This is reflected by the very poor agreement between R_i and R_{ii}. All further experiments were conducted at a MAS spinning speed of 5 kHz.

Table 2 reports the relaxation-rate matrix of DMPC calculated according to the three different approaches. Most cross-relaxation rates calculated by the pair interaction approach are indistinguishable from values calculated by the matrix approach. However, for some smaller rates, the pair interaction approach reports values which are systematically higher. Application of the pair interaction approach must be restricted to the more intense resonance peaks in the spectrum. The rates calculated by the single mixing time approach are less reliable and report qualitative features of magnetization exchange only.

So far, we reported only the magnetization transfer between the resonances in the centerband. However, magnetization may also be transferred from resonance centerbands to all sidebands. These transfers are part of the overall magnetization transfer between resonances and must be accounted for. We determined cross-relaxation rates to the first sidebands experimentally at a spinning speed of 5 kHz by acquiring spectra with an increased spectral width. The rates were determined by the pair interaction approach. Overall, the center-to-first sideband transfers resulted in minor corrections to total cross-relaxation rates only. As expected, the cross-relaxation rates between the centerband and the first sideband of glycerol and upper hydrocarbon chain resonances are highest with values of 10−15% of the corresponding rates between the centerband signals. The other center-to-sideband rates are only a few percent of the corresponding rates in the centerband. In the following, only the cross-relaxation rates within the centerband have been analyzed.

Intermolecular contribution to NOESY Cross-Relaxation. To determine the amount of intermolecular cross-relaxation, the protonated DMPC was mixed with DMPC-d_{67} which is deuterated in all positions except the glycerol backbone and the partially (∼50%) deuterated C-2 methylene groups of both hydrocarbon chains. Dilution of the protonated DMPC in the deuterated matrix increased spin−lattice relaxation times, confirming that intermolecular dipole−dipole interactions contribute to T_1 relaxation, especially for those groups with the largest order parameters (Table 3).

Figure 5 shows typical dependencies of cross-relaxation rates as a function of the mole fraction of perdeuterated lipid in the mixture. Behavior can be categorized into two subgroups. (i) *Partial intermolecular cross-relaxation*: The cross-relaxation rate decreases linearly to a residual intramolecular rate of a finite

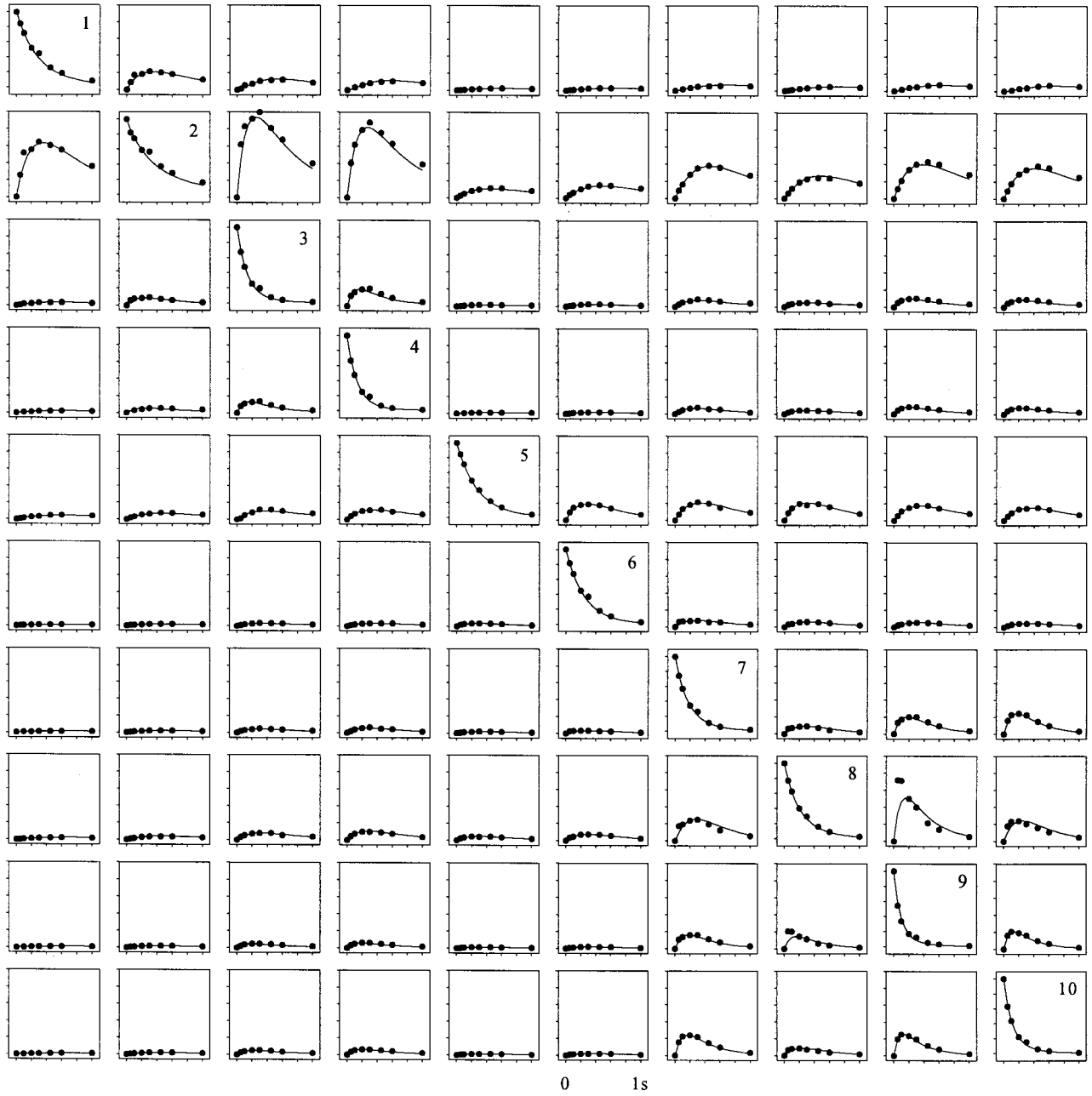

Figure 4. Mixing time dependence of all diagonal peaks and cross-peaks of DMPC. For plotting purposes, the peak volumes were scaled to unity by the matrix $\mathbf{a}(t_m) = \mathbf{A}(t_m)\,\mathbf{A}(0)^{-1}$. Horizontal axes of individual frames represent the mixing time from 0 to 1 s, and the vertical axes represent the diagonal peak volumes from 0 to 1 and the cross-peak volumes from 0 to 0.35 in relative units. Filled circles show measured peak volumes, and solid lines represent a fit to the data points using the parameters from resolving matrix equation (4).

value as the mole fraction of DMPC-d_{67} increases (Figure 5A). This applies to lipid resonances, which are nearest-neighbors by chemical bond. (ii) *Entirely intermolecular cross-relaxation*: The cross-relaxation rate decreases to zero with increasing amounts of deuterated lipid in the mixture (Figure 5B). Case ii applies to the majority of lipid resonances. Figure 5C reports cross-relaxation rates between glycerol signals, which are not deuterated in DMPC-d_{67} and, therefore, do not change. Magnetization exchange in cases where only the magnetization emitting or receiving site is deuterated is more complex. Figure 5D reports cross-relaxation from the always-protonated glycerol to the increasingly deuterated headgroup signal where deuteration reduces cross-relaxation rates to zero. However, the reverse rate of transfer from the remaining protons in the headgroup to the always-protonated glycerol is constant, because the probability of a headgroup proton encountering the always-protonated glycerol protons has not changed. Finally, Table 4 shows the amount of intermolecular cross-relaxation between all resolved lipid resonances in percent.

Because the proton signals of the two lipid hydrocarbon chains are superimposed, magnetization transfer between chain lipid signals may occur inside one chain and between the two chains in the same lipid. From comparison of cross-relaxation rates in a 10/90 (mol/mol) mixture of single-chain-deuterated DMPC-d_{27} and DMPC-d_{67}, it was determined that about 20−30% of the intramolecular cross-relaxation occurs between the two chains of a lipid molecule.

Discussion

Quantitative Analysis of Cross-Relaxation Data. Application of the matrix approach allowed the determination of cross-

TABLE 1: Peak Assignments and Spin−Lattice Relaxation Rates of DMPC at Several Spinning Speeds at 30 °C

				R_i (s^{-1}) (inversion−recovery)			R_{ii} (s^{-1}) (NOESY)		
peak	assignment[a]	chemical shift (ppm)	no. of protons	2.5 kHz	5 kHz	10 kHz	2.5 kHz	5 kHz	10 kHz
1	CH_3	0.89	6	1.06	1.16	1.05	2.23	1.48	0.94
2	(CH_2)$_n$	1.30	40	1.33	1.45	1.46	1.65	1.42	0.82
3	CH_2−CH$_2$−CO	1.60	4	1.56	1.66	1.63	−0.48	1.27	1.32
4	CH_2−CO	2.37	4	1.58	1.65	1.63	2.20	1.32	1.15
5	N−(CH_3)$_3$, γ	3.23	9	2.01	2.03	2.24	2.92	2.86	2.52
6	CH_2−N, β	3.68	2	1.95	1.94	2.04	3.01	2.47	2.40
7	CH_2−OP, G-3	3.99	2	1.61	1.61	1.60	−0.42	0.62	0.96
8	PO−CH_2, α and OCO−CH_2, G-1	4.21	2 + 1	1.61	1.70	1.66	2.77	1.77	1.52
9	OCO−CH_2, G-1	4.44	1	1.60	1.66	1.55	2.01	1.01	0.82
10	OCO−CH, G-2	5.28	1	1.54	1.52	1.37	4.48	2.20	1.41

[a] The peak assignments were taken from Holte and Gawrisch.[24]

TABLE 2: Relaxation Matrices for Pure DMPC[a]

	1	2	3	4	5	6	7	8	9	10
peak (ppm)	0.89	1.30	1.60	2.37	3.23	3.68	3.99	4.21	4.44	5.28
1	3.4[b]	−0.59[c]	−0.066	−0.031	−0.031	−0.034	−0.062	−0.042	−0.068	−0.032
		−0.62[d]	−0.22	−0.15	−0.032	−0.044	−0.084	−0.059	−0.095	−0.072
		−0.54[e]	−1.09	−0.7	−0.052	−0.059	−0.21	−0.16	−0.54	−0.4
2	−1.78	2.93	−3.85	−3.08	−0.22	−0.27	−0.66	−0.44	−1.02	−0.79
	−2.12		−5.56	−3.43	−0.21	−0.28	−0.76	−0.49	−0.95	−0.79
	−1.86		−8.71	−7.8	−0.28	−0.39	−1.73	−0.89	−3.81	−3.09
3	−0.019	−0.36	7.13	−1.17	−0.037	−0.069	−0.22	−0.14	−0.53	−0.42
	−0.06	−0.36		−0.91	−0.035	−0.063	−0.22	−0.15	−0.37	−0.32
	−0.11	−0.24		−1.45	−0.037	−0.055	−0.31	−0.16	−0.84	−0.65
4	−0.006	−0.2	−0.79	7.18	−0.032	−0.049	−0.24	−0.14	−0.49	−0.38
	−0.029	−0.18	−0.61		−0.03	−0.044	−0.23	−0.15	−0.35	−0.3
	−0.041	−0.13	−0.89		−0.022	−0.039	−0.34	−0.16	−0.74	−0.61
5	−0.06	−0.14	−0.26	−0.32	3.57	−0.64	−0.59	−0.68	−0.43	−0.43
	−0.063	−0.14	−0.24	−0.3		−0.68	−0.62	−0.65	−0.49	−0.33
	−0.1	−0.16	−0.76	−0.74		−0.78	−1.02	−0.95	−1.6	−1.56
6	−0.012	−0.033	−0.088	−0.092	−0.12	4.01	−0.25	−0.2	−0.15	−0.14
	−0.016	−0.033	−0.08	−0.082	−0.12		−0.33	−0.2	−0.16	−0.14
	−0.019	−0.036	−0.18	−0.21	−0.13		−0.36	−0.25	−0.47	−0.4
7	−0.01	−0.035	−0.12	−0.2	−0.048	−0.11	5.66	−0.28	−1.11	−1.39
	−0.013	−0.04	−0.13	−0.19	−0.051	−0.15		−0.41	−1.01	−1.36
	−0.016	−0.037	−0.24	−0.42	−0.038	−0.084		−0.32	−1.87	−1.75
8	−0.019	−0.065	−0.22	−0.33	−0.16	−0.25	−0.76	4.9	−3.16	−0.86
	−0.027	−0.055	−0.24	−0.34	−0.15	−0.25	−1.15		−9.02	−1.39
	−0.051	−0.082	−0.53	−0.85	−0.16	−0.25	−1.4		−4.33	−2.3
9	−0.009	−0.044	−0.24	−0.33	−0.028	−0.055	−0.89	−0.91	9.91	−1.59
	−0.012	−0.039	−0.17	−0.23	−0.032	−0.058	−0.8	−1.99		−1.41
	−0.019	−0.038	−0.31	−0.43	−0.029	−0.051	−0.87	−0.47		−1.53
10	−0.005	−0.041	−0.23	−0.31	−0.035	−0.061	−1.37	−0.3	−1.94	8.23
	−0.011	−0.04	−0.18	−0.24	−0.034	−0.063	−1.33	−0.48	−1.74	
	−0.019	−0.043	−0.32	−0.5	−0.038	−0.061	−1.13	−0.35	−2.11	

[a] Rate constants are given in s^{-1}. [b] Diagonal relaxation rate calculated by the matrix approach. [c] Cross-relaxation rate by the matrix approach. [d] Cross-relaxation rate calculated by the pair interaction model. [e] Cross-relaxation rate calculated from a NOESY experiment at a mixing time of 300 ms.

TABLE 3: Relaxation Times (ms) of DMPC and DMPC/DMPC-d_{67} Mixtures at 30 °C

		DMPC		DMPC/DMPC-d_{67} (50/50, mol/mol)		DMPC/DMPC-d_{67} (10/90, mol/mol)	
peak	assignment	T_1	T_2	T_1	T_2	T_1	T_2
1	CH_3	862	39	913	33	1022	40
2	(CH_2)$_n$	692	16	743	15	839	22
3	CH_2−CH$_2$−CO	601	13	675	12	751	19
4	CH_2−CO	605	15	753	26	1105	42
5	N−(CH_3)$_3$	492	97	482	87	476	92
6	CH_2−N	515	51	536	41	534	49
7	CH_2−OP	623	18	706	14	826	15
8	PO−CH_2 and OCO−CH_2	589	46	603	38	856	23
9	OCO−CH_2	603	18	740	17	882	16
10	OCO−CH	659	31	737	27	923	28

relaxation and spin−lattice relaxation rates which described the mixing time dependence of diagonal peaks and cross-peaks in the two-dimensional NOESY spectra with very good precision (see Figure 4). Apparently, the uniform treatment of magnetization transfer by multiple protons underneath each resonance peak is a reasonable approximation. The minimum requirement in obtaining the relaxation-rate matrix is to conduct the experiment at two mixing times: a very short one to obtain diagonal peak intensities before any exchange of magnetization has occurred and a longer time at which the cross-peaks have almost maxi-

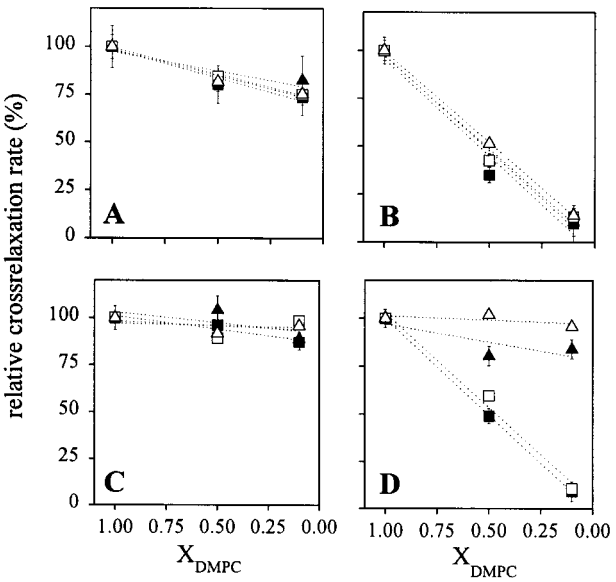

Figure 5. Relative changes in cross-relaxation rates as a function of the mole fraction of DMPC in the DMPC/DMPC-d_{67} mixtures calculated by the matrix approach (■, ▲) and the pair interaction model (□, Δ). Rates for pure DMPC were set to 100%. Both cross-relaxation rates σ_{ij} (■, □) and σ_{ji} (▲, Δ) are shown. Error bars are available only for the data calculated by the pair interaction model. Panel A shows the rates between $-(CH_2)_n-$ and $-CH_2-C-CO-$ resonance peaks of the chains that are 70% intramolecular. Panel B shows the exclusively intermolecular rate between chain $-(CH_2)_n-$ and headgroup $-N(CH_3)_3$ resonances. Panel C shows rates between the nondeuterated glycerol resonances. Panel D shows the rate between the increasingly deuterated $N(CH_3)_3-$ headgroup protons and the always-protonated glycerol G-3 protons (see Results section for interpretation).

mum intensity. However, precision of analysis must be confirmed by plotting the matrix solution to the data from six to eight experiments conducted at different mixing times (see Figure 4).

The pair interaction model was applied in parallel (see data in Table 2) to establish if analysis of pairs of diagonal peaks and the cross-peaks between them provides reliable cross-relaxation data. For high and intermediate cross-relaxation rates between intense diagonal peaks, the pair interaction approach gives results that are indistinguishable from the full matrix approach. However, the pair interaction model performs poorly for lower rates of transfer, i.e., in peaks which also have large transfer to other resonances. In particular, the cross-relaxation rates between neighboring protons in lipid hydrocarbon chains are very high, which interferes with the calculation of magnetization transfer between chain protons which are more distant.

The single mixing time analysis is a suitable alternative when relative rate differences between structurally close lipid systems are compared. Data should be obtained at a short mixing time to avoid the perturbing influence from spin−lattice relaxation. The approach may result in systematic deviations between data sets with substantial differences in proton spin−lattice relaxation. Furthermore, the same limitations as for the pair interaction model regarding the dynamic range of cross-relaxation rates apply to this approach.

In summary, the matrix approach provides the highest quality of data analysis. It is feasible to analyze magnetization transfer in truncated matrices as long as the most intense diagonal peaks and cross-peaks are included. Weaker interactions can be ignored without harm to the precision of calculated cross-relaxation rates. This observation could be of practical importance, because it may not be possible to analyze the entire set of cross-relaxation rates in every experiment.

Intra- vs Intermolecular Cross-Relaxation. Dilution of protonated DMPC in perdeuterated DMPC-d_{67} reduced cross-relaxation rates between distant protons in the lipid to zero (see Table 4). There is no measurable magnetization transfer within the same lipid molecule, except between protons that are neighbors by chemical bond. The spin pools of the lipid headgroup, the glycerol, the upper chain segments, and the terminal chain methyl groups are effectively isolated, and the transfer of magnetization between these pools occurs exclusively by direct intermolecular interactions. This result proves that there is no magnetization transfer by spin diffusion over several bonds within the DMPC molecule. Qualitative validation of the intermolecular nature of some of these transfers had been presented by other laboratories.[4,6,9,10] However, previous results failed to highlight the full extent of intermolecular cross-relaxation in lipid bilayers. The absence of any measurable magnetization transfer over several bonds within the same DMPC molecule is also an indication that chain upturns, if they should occur, do not result in the close approach of lipid segments in the same molecule.

Comparison of magnetization transfer of DMPC in DMPC-d_{67} versus single-chain-deuterated DMPC-d_{27} in DMPC-d_{67} revealed that approximately 10−20% of the magnetization transfer between chain resonances occurs between the two chains within the same lipid molecule. This range is in reasonable agreement with the value of 16.7% calculated by assuming that lipid hydrocarbon chains form a hexagonal lattice in which every chain is surrounded by six other chains.

Cross-Relaxation Rates and Bilayer Structure. Interpretation of cross-relaxation rates has to account for the multitude of molecular contacts between neighboring lipid molecules. In the bilayer, a first coordination shell of lipids surrounds every phospholipid molecule. The average lifetime of a lipid molecule in this coordination shell can be estimated from the lateral diffusion constant of lipids in the bilayer,[22] which is $D = 1 \times 10^{-8}$ cm^2/s. If we assume that a molecule has to travel on the order of 8 Å to replace a molecule in the coordination shell, then the average lifetime of a molecule in this shell is about 100 ns. Protonated DMPC and deuterated DMPC-d_{67} behave like an ideal mixture, and the probability of having two protonated lipids as nearest-neighbors decreases proportionally to the DMPC concentration. In perfect agreement with this model, the cross-relaxation rates in the DMPC/DMPC-d_{67} mixture decrease linearly with decreasing DMPC content.

Furthermore, cross-relaxation rates are modulated by faster motions of interacting lipid segments with correlation times on the order of 1 ns. These are the diffusive rotational and tumbling motions of the entire lipid molecule, as well as the structural isomerization and librational motions within the lipid. The autocorrelation functions of the magnetic dipole−dipole interactions between the protons that are sufficiently close (<5 Å) depend on the variation of proton distances and the angular fluctuations of the distance vector. Although we are currently unable to analyze these autocorrelation functions, the experimental data suggest that they do not vary much between interaction of different lipid segments. To demonstrate this, we divided the membrane into four regions—methyl end of hydrocarbon chain, upper hydrocarbon chain, glycerol, and headgroup—and we selected a typical resonance for each region. Approximate cross-relaxation rates per interacting proton were calculated by dividing the rates in Table 2 by the number of magnetization acceptor protons. This normalization corrects for the different number of protons underneath each resonance and allows comparison of cross-relaxation rates over the entire

TABLE 4: Percentage of Intermolecular Contribution to DMPC Cross-Relaxation Rates

cross-peak	% intermolecular	cross-peak	% intermolecular	cross-peak	% intermolecular
$CH_3 \times (CH_2)_n$	40−60[a]	$(CH_2)_n \times$ G-1	100	$\gamma \times \beta$	60−70
$CH_3 \times CH_2-C-CO$	100	$(CH_2)_n \times$ G-2	100	$\gamma \times$ G-3	100
$CH_3 \times CH_2-CO$	100	$CH_2-C-CO \times CH_2-CO$	60	$\gamma \times \alpha$, G-1	65
$CH_3 \times \gamma$	100	$CH_2-C-CO \times \gamma$	100	$\gamma \times$ G-1	100
$CH_3 \times \beta$	100	$CH_2-C-CO \times \beta$	100	$\gamma \times$ G-2	100
$CH_3 \times$ G-3	100	$CH_2-C-CO \times$ G-3	100	$\beta \times$ G-3	75
$CH_3 \times \alpha$, G-1	100	$CH_2-C-CO \times \alpha$, G-1	100	$\beta \times \alpha$, G-1	80
$CH_3 \times$ G-1	100	$CH_2-C-CO \times$ G-1	100	$\beta \times$ G-1	95−100
$CH_3 \times$ G-2	100	$CH_2-C-CO \times$ G-2	100	$\beta \times$ G-2	100
$(CH_2)_n \times CH_2-C-CO$	25−30[b]	$CH_2-CO \times \gamma$	100	G-3 $\times \alpha$, G-1	N/A
$(CH_2)_n \times CH_2-CO$	100	$CH_2-CO \times \beta$	100	G-3 $\times$ G-1	N/A
$(CH_2)_n \times \gamma$	100	$CH_2-CO \times$ G-3	N/A[c]	G-3 $\times$ G-2	N/A
$(CH_2)_n \times \beta$	90−100	$CH_2-CO \times \alpha$, G-1	N/A	α, G-1 $\times$ G-1	N/A
$(CH_2)_n \times$ G-3	100	$CH_2-CO \times$ G-1	N/A	α, G-1 $\times$ G-2	N/A
$(CH_2)_n \times \alpha$, G-1	100	$CH_2-CO \times$ G-2	N/A	G-1 $\times$ G-2	N/A

[a] About 20% of the intramolecular cross-relaxation occurs between the two chains of the molecule. [b] About 30% of the intramolecular cross-relaxation occurs between the two chains of the molecule. [c] Not available because of protonated glycerol or partially protonated C_2 methylene groups in DMPC-d_{67}.

TABLE 5: Intermolecular Cross-Relaxation Rates (s^{-1}) per Proton between Segments of DMPC Molecules in Bilayers[a]

	upper chain[b]	glycerol[c]	headgroup[d]
end of chain[e]	−0.008	−0.005	−0.006
upper chain[b]		−0.17	−0.02
glycerol[c]			−0.07
headgroup[f]			−0.06

[a] Per proton rates were calculated by dividing the cross-relaxation rates by the number of magnetically equivalent "receiving" protons. The following lipid resonances were used: (See Table 1 for assignments.) [b] Peak 3. [c] Peak 10. [d] Peak 5. [e] Peak 1. [f] Peak 6.

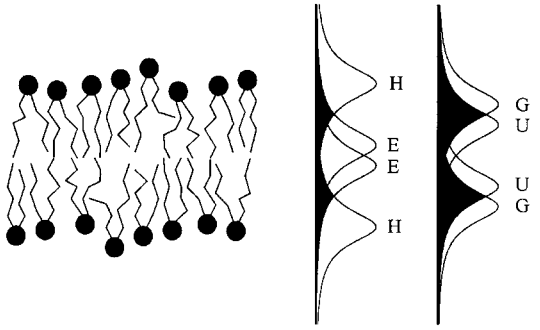

Figure 6. Intramolecular conformational transitions and intermolecular disorder in lipid membranes resulting in frequent contacts between all segments of lipid molecules. According to our model, magnetization transfer represents the frequency of collisions between lipid segments. The probability of collisions depends on the overlap of the spatial distribution functions of lipid segments. Two hypothetical distributions are shown on the right side. Because of intermolecular disorder, the glycerol (G) and upper chain (U) lipid regions significantly overlap in distribution functions, which results in high cross-relaxation rates between protons of these lipid segments. Much less overlap in location occurs between the headgroup protons (H) and the protons at the end of the hydrocarbon chains (E), which translates into cross-relaxation rates that are an order of magnitude smaller.

bilayer. The "normalized" proton−proton cross-relaxation rates are reported in Table 5. These rates differ by a maximum of about a factor of 30 throughout the bilayer. Rates between groups with close distance, such as lipid glycerol and upper chain segments, are highest, and rates between more distant groups, such as headgroups and ends of chain, are lowest. The transfer rates between the methyl groups of choline and the terminal methyl groups of lipid hydrocarbon chains are about 1 order of magnitude smaller than transfer rates between choline and the nearby glycerol. It is tempting to suggest that the rates of intermolecular magnetization transfer depend foremost on the probability of close approach between two protons in the bilayer. The probability of locating a molecular group on an axis, *z*, which is the bilayer normal, is represented by a distribution function (Figure 6). Protons, which have significant overlap of their distribution densities along z, will approach each other frequently and, therefore, will have also the highest cross-relaxation rates, e.g., magnetization transfers from upper chain to glycerol. Distribution functions of more distant molecular groups have less overlap, and consequently, rates of magnetization transfer are lower.

Although we would like to interpret cross-relaxation rates solely in terms of close approach between lipid protons, it cannot be ruled out that different correlation times in lipid headgroup, glycerol, and chain regions influence rates of magnetization transfer to some extent. Preliminary results on the temperature dependence of intermolecular cross-relaxation rates suggest that cross-relaxation between lipids is determined primarily by rotational diffusion of the entire lipid molecule, with little influence from intramolecular conformational transitions. Cross-relaxation rates may also be influenced by differences in the proton distance of closest approach. However, it is unlikely that this distance varies because lipid molecules have a high degree of conformational freedom. The glycerol backbone region of lipids may be an exception because lipids are less flexible in this region.

Quantitative analysis of cross-relaxation rates between terminal methyl groups of hydrocarbon chains and the choline methyl groups shows that the probability of head-to-chain contacts is an order of magnitude lower than contacts between less distant groups, indicating that the integrity of the lipid bilayer arrangement with headgroups near the interface and end of chains in the bilayer center is maintained. Nevertheless, these substantial rates of magnetization transfer and the even higher rates between less distant protons suggest that shifts in location of neighboring lipid segments by several angstroms along the bilayer normal are very likely. Even by conservative estimates, the rates between ends of chains and ends of headgroups are much higher than current models of the lipid bilayer would predict. Structural isomerization in lipid headgroups and the terminal methyl region of hydrocarbon chains is particularly fast. Therefore, it is much more likely that differences in lipid dynamics lower the cross-relaxation rates between these distant lipid segments, compared to models that ignore differences in lipid dynamics. In any event, this is a reminder that mem-

branes are highly dynamic structures with significant molecular disorder.

Another implication of this work is that cross-relaxation rates contain valuable information about *lateral* organization of lipid species in the membrane. Cross-relaxation rates report true statistics of nearest-neighbor contacts in the bilayer. Provided that unique resonance signals for a particular lipid are available, the formation of liquid crystalline clusters of lipids can be investigated via cross-relaxation rates. We have used this technique to study the influence of chain unsaturation and cholesterol on lateral lipid organization.[23] Furthermore, determination of cross-relaxation rates between lipids and molecules incorporated into lipid bilayers as ethanol[24] or indole analogues[25] aids in locating these molecules in the membrane.

Acknowledgment. D.H. is grateful for a grant by the Studienstiftung des deutschen Volkes. K.A. and D.H. acknowledge support by the Deutsche Forschungsgemeinschaft (SFB 197).

References and Notes

(1) Wiener, M. C.; White, S. H. *Biophys. J.* **1992**, *61*, 434−447.
(2) Petrache, H. I.; Gouliaev, N.; Tristram-Nagle, S.; Zhang, R.; Suter, R. M.; Nagle, J. F. *Phys. Rev. E* **1998**, *57*, 7014−7024.
(3) Singer, S. J.; Nicolson, G. L. *Science* **1972**, *175*, 720−731.
(4) Forbes, J.; Bowers, J.; Shan, X.; Moran, L.; Oldfield, E.; Moscarello, M. A. *J. Chem. Soc., Faraday Trans. 1* **1988**, *84*, 3821−3849.
(5) Forbes, J.; Husted, C.; Oldfield, E. *J. Am. Chem. Soc.* **1988**, *110*, 1059−1065.
(6) Xu, Z.-C.; Cafiso, D. S. *Biophys. J.* **1986**, *49*, 779−783.
(7) Gabriel, N. E.; Roberts, M. F. *Biochemistry* **1987**, *26*, 2432−2440.
(8) Halladay, H. N.; Stark, R. E.; Ali, S.; Bittman, R. *Biophys. J.* **1990**, *58*, 1449−1461.
(9) Volke, F.; Pampel, A. *Biophys. J.* **1995**, *68*, 1960−1965.
(10) Chen, Z. J.; Stark, R. E. *Solid State Nucl. Magn. Reson.* **1996**, *7*, 239−246.
(11) Brown, M. L.; Venable, R. M.; Pastor, R. W. *Biopolymers* **1995**, *35*, 31−46.
(12) Pastor, R. W.; Feller, S. E. In *Biological Membanes*: *A Molecular Perspective from Computation and Experiment*; Merz, K. M., Roux, B., Eds.; Birkhäuser: Boston, 1996; pp 3−30.
(13) Beall, P. T.; Amtey, S. R.; Kasturi, S. R. *NMR Data Handbook for Biomedical Applications*; Pergamon Press: New York, 1984; pp 32−39.
(14) Jeener, J.; Meier, B. H.; Bachmann, P.; Ernst, R. R. *J. Chem. Phys.* **1979**, *71*, 4546−4553.
(15) Wagner, G.; Wüthrich, K. *J. Mol. Biol.* **1982**, *155*, 347−366.
(16) Ernst, R. R.; Bodenhausen, G.; Wokaun, A. *Principles of Nuclear Magnetic Resonance in One and Two Dimensions*; Clarendon Press: Oxford, 1987.
(17) Perrin, C. L.; Gipe, R. K. *J. Am. Chem. Soc.* **1984**, *106*, 4036−4038.
(18) Bremer, J.; Mendz, G. L.; Moore, W. J. *J. Am. Chem. Soc.* **1984**, *106*, 4691−4696.
(19) Macura, S.; Ernst, R. R. *Mol. Phys.* **1980**, *41*, 95−117.
(20) Seelig, J. *Q. Rev. Biophys.* **1977**, *10*, 353−418.
(21) Brown, L. R.; Farmer, B. T., II. *Methods Enzymol.* **1989**, *176*, 199−216.
(22) Wu, E. S.; Jacobson, K.; Papahadjopoulos, D. *Biochemistry* **1977**, *16*, 3836−3841.
(23) Huster, D.; Arnold, K.; Gawrisch, K. *Biochemistry* **1998**, in press.
(24) Holte, L. L.; Gawrisch, K. *Biochemistry* **1997**, *36*, 4669−4674.
(25) Yau, W.-M.; Wimley, W. C.; Gawrisch, K.; White, S. H. *Biochemistry* **1998**, *37*, 14713−14718.